Journal of Cerebral Blood Flow & Metabolism (2010) 30, 883–894

www.jcbfm.com

Early nonischemic oxidative metabolic dysfunction leads to chronic brain atrophy in traumatic brain injury

Yueqiao Xu[4], David L McArthur[1], Jeffry R Alger[2], Maria Etchepare[1], David A Hovda[1], Thomas C Glenn[1], Sungcheng Huang[3], Ivo Dinov[1] and Paul M Vespa[1,2]

[1]*Department of Neurosurgery, David Geffen School of Medicine, University of California at Los Angeles, Los Angeles, California, USA;* [2]*Department of Neurology, David Geffen School of Medicine, University of California at Los Angeles, Los Angeles, California, USA;* [3]*Department of Molecular and Medical Pharmacology, and UCLA-DOE Center for Molecular Medicine, David Geffen School of Medicine, University of California at Los Angeles,Los Angeles, California, USA;* [4]*Department of Neurosurgery, Xuanwu Hospital, Capital Medical University, Beijing, China*

Chronic brain atrophy after traumatic brain injury (TBI) is a well-known phenomenon, the causes of which are unknown. Early nonischemic reduction in oxidative metabolism is regionally associated with chronic brain atrophy after TBI. A total of 32 patients with moderate-to-severe TBI prospectively underwent positron emission tomography (PET) and volumetric magnetic resonance imaging (MRI) within the first week and at 6 months after injury. Regional lobar assessments comprised oxidative metabolism and glucose metabolism. Acute MRI showed a preponderance of hemorrhagic lesions with few irreversible ischemic lesions. Global and regional chronic brain atrophy occurred in all patients by 6 months, with the temporal and frontal lobes exhibiting the most atrophy compared with the occipital lobe. Global and regional reduction in cerebral metabolic rate of oxygen ($CMRO_2$), cerebral blood flow (CBF), oxygen extraction fraction (OEF), and cerebral metabolic rate of glucose were observed. The extent of metabolic dysfunction was correlated with the total hemorrhage burden on initial MRI ($r = 0.62$, $P = 0.01$). The extent of regional brain atrophy correlated best with $CMRO_2$ and CBF. Lobar values of OEF were not in the ischemic range and did not correlate with chronic brain atrophy. Chronic brain atrophy is regionally specific and associated with regional reductions in oxidative brain metabolism in the absence of irreversible ischemia.
Journal of Cerebral Blood Flow & Metabolism (2010) **30,** 883–894; doi:10.1038/jcbfm.2009.263; published online 23 December 2009

Keywords: atrophy; metabolism; MRI; positron emission tomography; traumatic brain injury

Introduction

Traumatic brain injury (TBI) is a major cause of death and severe morbidity worldwide (Langlois *et al*, 2003). It results in immediate cellular death in a limited region of the brain directly involved in the insult, usually a brain contusion, while creating a more widespread state of metabolic dysfunction in remote areas of the brain (Feeney and Baron, 1986). Secondary cell loss takes the form of chronic diffuse atrophy in regions not directly involved in the primary injury or adjacent to the primary contusion (Marcoux *et al*, 2008). Chronic brain atrophy has been correlated with poor neurologic outcome (Sidaros *et al*, 2009) and seems to be progressive over a period ranging from months to years after the injury. The causes of atrophy are not well understood, and thereby limit efforts to secondarily prevent the process. This paper investigates the potential role of brain metabolism in the first week after injury in chronic brain atrophy.

Volumetric magnetic resonance imaging (MRI) studies of chronic TBI (Sidaros *et al*, 2009; Trivedi *et al*, 2007; Levin *et al*, 2000; Tate and Bigler, 2000; Verger *et al*, 2001; Yount *et al*, 2002) have reported

Correspondence: Dr PM Vespa, Departments of Neurosurgery and Neurology, David Geffen School of Medicine at UCLA, Ronald Reagan UCLA Medical Center, 757 Westwood Blvd, Room RR 6236A, Los Angeles, CA 90095, USA.
E-mail: PVespa@mednet.ucla.edu
The research was supported by Grant nos NS049471, NS02089, and the California State Neurotrauma Initiative.
Received 17 August 2009; revised 26 October 2009; accepted 18 November 2009; published online 23 December 2009

that global and regional brain atrophy occurs over a period ranging from months to years after the injury. This atrophy seems to be dependent on the extent of the initial injury, can involve important structures such as the hippocampus, and correlates with deficits in long-term cognitive performance (Wilde *et al*, 2005; Levine *et al*, 2008). The mechanisms involved in this chronic atrophy have not been well studied. In an initial study (Marcoux *et al*, 2008), our group at UCLA (University of California at Los Angeles) evaluated the role of early metabolic dysfunction on subsequent brain atrophy. The principal finding was that the duration of persistent metabolic crisis as measured by the elevated lactate–pyruvate ratio is associated with the extent of regional frontal lobe atrophy. This result suggested that early brain metabolism was one determinant factor in chronic brain atrophy.

These results led us to hypothesize that the extent of regional brain atrophy is related to that of metabolic dysfunction, specifically to the reduction in oxidative metabolism. To investigate this possibility, we prospectively evaluated multiple lobar regions of the brain using positron emission tomography (PET) combined with volumetric MRI performed during the initial week after TBI, and compared these measures using coregistration techniques with chronic volumetric MRI in a within-subjects design.

Materials and methods

Patient Population

This study was approved by our Institutional Review Board and was conducted as part of the UCLA Brain Injury Research Center in patients with TBI. The main inclusion criteria were as follows: (1) a Glasgow Coma Scale (GCS) score of ≤ 8 or a GCS of 9 to 15 with computerized tomography brain scans showing intracranial bleeding; (2) sufficient medicophysiologic stability to perform PET and MRI scans in the acute period; (3) follow-up MRI 6 months after the primary injury; and (4) image quality sufficient for evaluation. Surrogate informed consent was obtained. A total of 32 patients were enrolled and subsequently studied with PET, as well as acute and long-term MRI. In all, 12 age-matched uninjured volunteers were also recruited for comparison.

General Management Protocol

The management protocol was outlined previously (Vespa *et al*, 2005). Briefly, all patients were admitted to the neurointensive care unit after initial stabilization in the emergency room or after surgery. Craniotomies were performed for evacuation of intracranial mass lesions and hematomas. Intracranial pressure (ICP), measured by ventriculostomy, was maintained below 20 mm Hg using a standardized treatment protocol including head of bed up to 30°, mild hyperventilation ($PaCO_2 = 30$ to 35 mm Hg), external ventriculostomy with cerebrospinal fluid drainage, moderate sedation with low doses of propofol, normoglycemia (80 to 120 mg/dL), and maintenance of mild hypernatremia (sodium = 140 to 145 mmol/L). Refractory ICP was managed by pentobarbital-induced burst suppression coma. Cerebral perfusion pressure was kept above 60 mm Hg with volume repletion and vasopressors. Continuous jugular venous oxygen saturation was monitored and kept at 60% to 70% through adjustments in cerebral perfusion pressure. Continuous electroencephalographic monitoring was performed to assess the presence of seizure activity and to monitor the effect of barbiturates when burst suppression was induced.

Positron Emission Tomography Protocol

Positron emission tomography was performed using a quantitative method described previously (Bergsneider *et al*, 2001; Wu *et al*, 2004). Patients were placed in the scanner and physiologic monitoring of ICP, end-tidal CO_2, arterial blood gases, arterial blood pressure, continuous electroencephalography, core temperature, and heart rate were monitored using a portable intensive care unit monitoring system. These physiologic parameters were kept similar to those present in the intensive care unit. Intracranial pressure was kept under 20 mm Hg, CO_2 was kept at 30 to 34 mm Hg, and temperature was maintained between 37.0°C and 37.6°C. Patients underwent serial O-15 PET scans ($C^{15}O$, $O^{15}O$, $H_2^{15}O$) using dynamic blood sampling to determine regional cerebral blood flow (CBF, expressed as ml per (100 g/min)), oxygen extraction fraction (OEF, %), and cerebral metabolic rate of oxygen ($CMRO_2$, ml per (100 g/min)). Images of OEF were generated using the initial 5 mins of the $O^{15}O$ study and were assessed by a compartmental model for oxygen that accounts for recirculated $H_2^{15}O$ (Ohta *et al*, 1992). The $O^{15}O$ raw images (voxel size: $1.471 \times 1.471 \times 2.45\ mm^3$) were smoothed using a three-dimensional filter (in plane full-width at half-maximum = 2.942 mm, axial full-width at half-maximum = 2.45 mm) before OEF images were generated on a voxel basis. This was followed by a 2-Deoxy-2-[18F] fluoro-D-Glucose PET scan obtained using a quantitative technique for the calculation of the regional cerebral metabolic rate of glucose (CMRglc, mg per (100 g/min)). Each brain PET scan contained 63 slices, and each brain lobe contained 20 to 30 slices. Coregistration with volumetric MRI was accomplished using a six-parameter rigid-body transformation program and visual evaluation (Lin *et al*, 1994) with realignment and partitioning. Four slices with equal intervals were selected, and the regions of interest (ROIs) of the brain lobe were drawn manually with the contusion areas excluded (Figure 1). The Means of the ROIs over four planes were calculated as lobe metabolic parameters. All analyses were carried out using Janus Program version 6.3 (Los Angeles, CA, USA; http://149.142.143.7/BIRC/INDEX.HTML).

Imaging and Volumetric Analysis

Acute and chronic (6-month) MRI studies were conducted using a Siemens Sonata 1.5 T MRI unit (Siemens, Munich, Germany). Acute and chronic MRI scans included volumetric T1-weighted MP-RAGE (Magnetization-Prepared Gradient Echo) imaging (MP-RAGE: TR (repetition time)

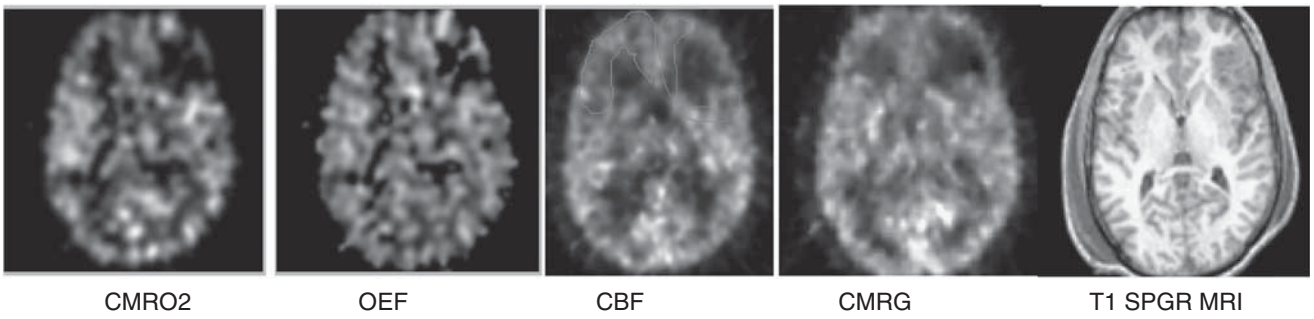

Figure 1 Comparison of coregistered acute MRI and PET images used for analysis. Regions of interest (ROIs) for each lobe were hand drawn for PET and MRI. An example of a single-slice ROI of the frontal lobe was drawn on the cerebral blood flow image to exclude the contusion on the left. $CMRO_2$, cerebral oxidative rate of oxygen; OEF, oxygen extraction fraction; CBF, cerebral blood flow; CMRG, cerebral metabolic rate of glucose.

1,900 msecs, echo time (TE) 3.5 msecs, FOV (field of view) 256×256, 1 mm slice thickness), axial FLAIR (fluid-attenuated inversion recovery imaging) (FLAIR: TR 9,590 msecs, TE 70 msecs, FOV 512×384, slice thickness 3 mm), axial diffusion weighted imaging (DWI: TR 6,000 msecs, TE 105 msecs, FOV 96×128, 7 mm slice, $b=0$ and 1,000 (3 directions), 1-scan trace) from which apparent diffusion coefficient (ADC) images were automatically calculated using the scanner software, and axial two-dimensional gradient recalled echo axial imaging (GRE: TR 1,500 msecs, TE 7 msecs, FOV 512×384, slice thickness 3 mm). The same MRI scanner was used for both acute and chronic imaging.

Volumetric T1-weighted MR images were analyzed using the following process. For lobar volume analysis, lobar ROIs were drawn using home-written plug-in software for ImageJ (NIH, Bethesda, MD, USA) 1.37 v (http://rsb.info.nih.gov)—to perform semi-automated lobar segmentation. Brainsuite Software (UCLA, Los Angeles, CA, USA) (Shattuck and Leahy, 2002) was used for final three-dimensional visualization. Images obtained using FLAIR were used to identify and exclude contusions. An ROI of each lobe was created using each of the relevant slices from the T1-weighted volume image. The dura mater, superior sagittal sinus, blood vessels, cranial nerves, and choroid plexus were excluded. Contusions were also excluded. Lobar boundaries were defined using a standard approach (Hayman, 1992) and an anatomic atlas (http://www.med.harvard.edu/AANLIB/cases/caseNA/pb9.htm). Examples of frontal lobe ROIs are provided in Figure 2. Lobar volumes were then determined using ImageJ, which counted the volume elements (voxels) in each lobar ROI, and multiplied by the voxel volume. Lobar volume measurements in chronic MRI were performed in the same manner, except that lobar ROIs from the acute study were used as a qualitative guide to exclude primary contusions. The primary contusion was judged to be the region containing a GRE hypointense lesion with a volume $>1\,cm^3$. To accommodate for inherent shift, due to reabsorbing blood and resolving macroscopic edema, careful attention was paid to anatomic landmarks, including the septum pellucidum, pineal gland, falx cerebri, sylvian fissure, and central sulcus. In this manner, a consistent verification of lobar geographic limits was maintained. An independent physician radiology expert blinded to the clinical data performed the volumetric measurements.

To control for brain edema, a separate independent computational approach used LONI Pipeline Software (UCLA, Los Angeles, CA, USA) (http://www.loni.ucla.edu/Software/Pipeline) as described by Dinov *et al* (2009) to measure whole brain volume for both acute and chronic time points in the patient and control groups. Volumetric T1-weighted MP-RAGE images were processed using an automated pipeline that (1) extracted brain volumes from the skull and scalp, (2) classified tissue voxels as background, normal gray matter (NGM), normal white matter or cerebrospinal fluid, and (3) measured brain volume as the sum of the normal gray matter and normal white matter voxel volumes. Images of the automatically generated volumes were manually checked for proper processing.

A search for acute ischemic injury occurring up to the time of MRI was conducted using a structured visual scoring approach for analysis of the DWI-ADC and GRE images. For this analysis, DWI-ADC and GRE image volumes were coregistered and all ADC hypointense lesions >0.1 cm in diameter were visually identified. An ischemic lesion was defined as any lesion with >0.1 cm diameter, which showed ADC reduced to a threshold of $\leq 550\,\mu m^2/sec$ without a reduction in GRE signal intensity. Diffuse axonal lesions were defined as lesions >0.1 cm in diameter in which ADC was $\leq 550\,\mu m^2/sec$ with GRE hypointensity. Lesions having hyperintense FLAIR signal and ADC increase in the absence of GRE hypointensity were considered ischemic lesions that had progressed beyond the acute stage. This criterion provided the highest possible sensitivity for detecting ischemic lesions. The ischemic lesion burden was determined for each subject. A specific search was conducted for DWI-ADC lesions in the border zone regions of the anterior and middle cerebral arteries, specifically to address small vessel ischemia that may have been precipitated during the early posttraumatic period because of to elevated ICP, hypotension, or hypoxemia.

Outcome Measures

Patients were contacted monthly by telephone by the study nurse to assess recovery status over a course of 6 months. Patients were also tested in person at 6 months using the GOS-e (extended Glasgow Outcome Scale) (Wilson *et al*, 1998).

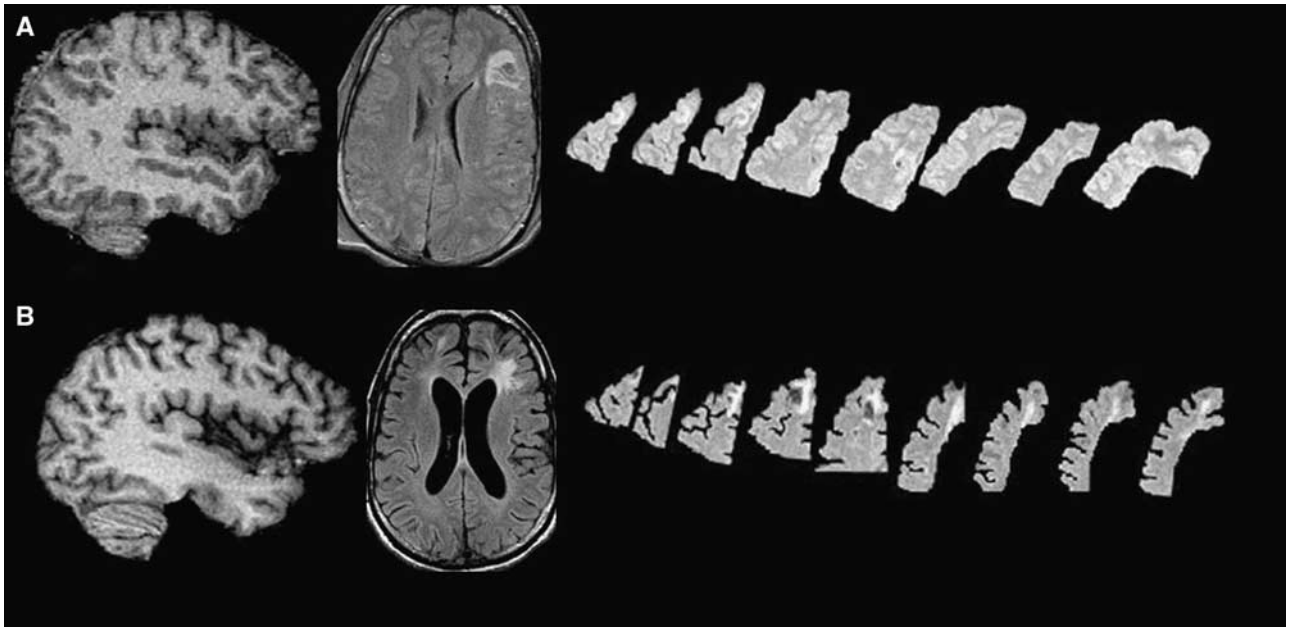

Figure 2 Example of ROI drawing for volume analysis. A two-example series of manual ROIs drawn using a stereotactic atlas (**A**, **B**) is shown. An overlapping cascade of frontal lobe ROIs drawn in the same patient outlined in Figure 1, with the orientation of superior to inferior as the images move from left to right. The acute scan is shown in panel A and the chronic scan in panel B.

Statistical Analysis

Statistical procedures were conducted using R version 2.9.1 (R Development Core Team, 2009). Statistical computations included mixed model analyses as well as Pearson's correlations and both conventional and robust *t*-tests. As the optimal confidence limits for bivariate Gaussian data are ellipses, these were calculated as per the results from the study by Goldberg and Iglewicz (1992), implemented in open-source R code by Wilcox (2005). Contour plots (Press *et al*, 1986) are shown by ellipses that are bivariate generalizations of M estimators. The inner ellipse contains 50% of the observations, directly analogous to the 1Q to 3Q (first quartile to third quartile) bounds within the traditional box plot, whereas the outer ellipse approximates the 99th percentile based on the ratio of the 99th to 50th percentiles of a χ^2 with 2 degrees of freedom.

Results

Patient Characteristics

A total of 32 patients were studied, with 28 men and 4 women. The mean age was 33 ± 15 years. The GCS distribution was skewed with 22/32 GCS total scores of >8. The mechanism of injury was blunt injury in most cases, with 22 motor vehicle accidents (69%) (including pedestrian or bicyclist hit by car), 6 falls (19%), 3 skateboarding accidents (14%), and 1 gunshot case (3%). Contusion with or without hematoma was found in 18 patients, contusion combined with subdural hematoma in 11, and contusion combined with epidural hematoma in 2 patients. Diffuse axonal shear hemorrhages were present in 30 cases. The PET study was conducted at a median of 5 days after trauma, acute MRI at a median of 8 days, and chronic MRIs at a median of 195 days after trauma. The mean GCS best score in 8 h after admission was 8. The mean GOS-e at 6-month follow-up was 5. Overall, 12 age- and gender-matched controls (mean age 31.8, male:female ratio 12:0) were included for comparison of global brain volumes (see Table 1).

A total of 11 patients underwent surgery within 24 h after trauma to evacuate a mass lesion and 2 of them had bones removed. Overall, 21 patients had intraventricular ICP monitoring, and 22 had $SJVO_2$ monitoring. Table 1 summarizes the demographic data of the study population and the longitudinal monitoring data with incidence of increased ICP, reduced cerebral perfusion pressure (CPP), and reduced jugular venous oxygenation ($SJVO_2$). Mean ischemia incidence was 0.5% ($SJVO_2 < 50\%$).

Ischemic and Hemorrhagic Lesion Structural Characterization

On acute MRI, measurements of ischemic and hemorrhagic lesions were performed. Isolated ischemic DWI-ADC lesions on MRI were seen in one subject, with lesions present diffusely in the white matter, corpus callosum, and arterial border zones between the anterior and middle cerebral arteries. In the remaining patients, DWI-ADC lesions were colocalized with the hemorrhagic shear lesions seen on GRE images. The number of hemorrhagic shear lesions ranged from 2 to 50 across subjects with a

mean diameter of 0.3 ± 0.2 cm. These were mostly confined to the white matter, centrum semiovale, thalamus, and the rims of extra-axial subdural hemorrhages. The DWI-ADC lesions were confined to the anatomic space of the hemorrhage in all but one case. In hemorrhagic lesions with $>5\,cm^3$ volume, a rim-like DWI-ADC restriction was seen in three patients. Figure 3 shows a single subject with ischemic DWI-ADC, and a representative subject with the more common finding of diffuse hemorrhagic injury.

Table 1 Demographic and longitudinal monitoring data

Trauma subject (n = *32*)	*Range*	*Mean* ± *s.d.*
Gender (male/female)	7	
Age (years)	16–81	33.4 ± 15.0
PET time (days)	1–16	5.4 ± 3.7
MRI acute (days)	1–19	7.8 ± 5.2
MRI chronic (days)	174–255	195 ± 19
GCS-8 h best score	3–15	7.6 ± 3.2
GOS-e 6 months	1–8	4.9 ± 1.6
ICP mean (mm Hg) ($n = 21$)	6–22	13.8 ± 3.3
CPP mean (mm Hg) ($n = 21$)	75–184	90.4 ± 22.3
$SJVO_2$ mean (%) ($n = 22$)	63–77	71.4 ± 3.8
% Time ICP >20	0–62	8.4 ± 13.3
% Time CPP <60	0–3	0.7 ± 0.9
% Time $SJVO_2$ <50%	0–3	0.7 ± 7
Normal control ($n = 12$)		
Gender (male/female)	12/0	
Age (years)	21–46	31.8 ± 9.7

GCS, Glasgow Coma Scale; GOS-e, extended Glasgow Outcome Scale; ICP, intracranial pressure; MRI, magnetic resonance imaging; PET, positron emission tomography.
Demographics of patient population and ICU physiology during the initial 96 h of monitoring.

Cerebral Metabolism in Acute Period Detected by Positron Emission Tomography

Table 2 presents PET parameters during the acute posttrauma period. Cerebral blood flow was low in all lobes but was significantly higher in the occipital lobes compared with the frontal and temporal lobes ($P = 0.004$ and $P = 0.017$, respectively). Oxidative metabolism was similarly low in all lobes without statistically significant differences between regions. Similarly, CMRglc was also low in all lobes. The OEF was low to normal in all lobes and not in the ischemic range when examined on a lobar or global basis.

Regional and Global Brain Atrophy

The mean volumes and atrophy of the different lobes are presented in Table 3. Significant change of volume of all lobes in acute and chronic MRI ($P = 0.001$ in all lobes) was detected using paired *t*-tests. Atrophy rates ranged from 0.03% to 37.15%, with a mean of 7.8 ± 7.2% in all lobes. Using a mixed model analyses, we found that chronic brain atrophy was greatest in the temporal ($P = 0.001$), parietal ($P = 0.016$), and frontal ($P = 0.038$) lobes in compari-

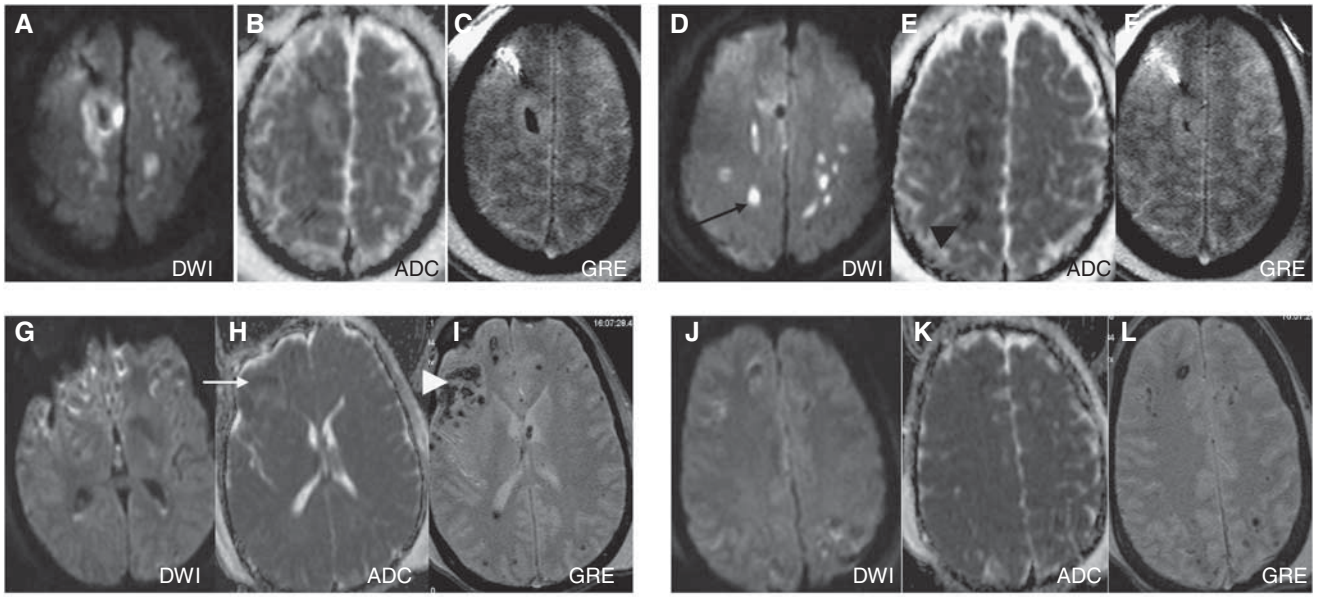

Figure 3 Example of structural lesion characterization: Two different patients are shown (**A**–**F**) and (**G**–**L**). Two separate axial slices per subject are shown with three image sequences per axial slice consisting of the DTI (left), DTA-ADC (middle), and GRE (right) in each sequence (panels A–F). The top row shows that the single patient had evidence of DTI-ADC hypointense (black arrowhead) and diffusion-weighted hyperintense lesions (black arrow) in the absence of obvious hemorrhage (panels C, F). The bottom row (E–H) shows an example of a patient with diffuse hemorrhagic lesions (white arrowhead) that colocalize with ADC (white arrow) and DWI areas. In 31 of 32 patients, DTI diffusion lesions were uniformly colocalized with GRE lesions as in panels G–L.

Table 2 Cerebral PET metabolism in acute period

Brain lobe	*CBF* (n = *64*) *(ml per (100 g/min))*	*OEF* (n = *64*) *(%)*	*$CMRO_2$* (n = *62*) *(ml per (100 g/min))*	*CMRglc* (n = *56*) *(ml per (100 g/min))*
Temporal	37.3 ± 11.9	38.0 ± 15.3	2.24 ± 0.87	3.23 ± 0.96
Frontal	36.3 ± 11.4	37.7 ± 15.7	2.13 ± 0.87	3.25 ± 1.06
Parietal	38.4 ± 11.4	37.7 ± 14.5	2.17 ± 0.86	3.23 ± 1.05
Occipital	43.4 ± 12.7	36.3 ± 14.0	2.41 ± 0.92	3.08 ± 0.96

CBF, cerebral blood flow; CMRglc, cerebral metabolic rate of glucose; $CMRO_2$, cerebral metabolic rate of oxygen; OEF, oxygen extraction fraction; PET, positron emission tomography.
Mean (±s.d.) values by region of oxidative metabolism ($CMRO_2$), CBF, glucose metabolism (CMRglc), and OEF.

Table 3 Acute and chronic brain lobar volumes

Brain lobe (n = *64*)	*Acute MRI* *(mm^3)*	*Chronic MRI* *(mm^3)*	*Contusion (mm^3)* *(number of involved lobes)*	*Atrophy* *(%)*	*Mixed effects*
Temporal	182,574 ± 26,572	164,905 ± 20,531	21,051 ± 19,259(26)	10.1 ± 7.7	0.003
Frontal	262,400 ± 44,777	243,962 ± 39,384	33,072 ± 31,247(30)	8.4 ± 8.6	0.04
Parietal	183,799 ± 31,289	170,592 ± 29,196	42,088 ± 42,597(7)	8.1 ± 6.6	0.016
Occipital	111,470 ± 17,293	106,790 ± 17,153	21,526 (1)	4.6 ± 4.0	NA

MRI, magnetic resonance imaging; NA, not applicable.
Mean (± s.d.) lobar brain volumes by region across all 32 patients. The *P*-value refers to the mixed effects model analysis.

son with the occipital lobes. Overall, the greatest extent of atrophy was seen in the temporal lobes (Table 3). Mean atrophy was 7.49 ± 4.27% in the left hemisphere and 7.66 ± 4.87% in the right, not significantly different ($P = 0.823$). The lobes with primary contusion had a mean of 13.1 ± 9.0% atrophy, significantly higher than the lobes without (6.0 ± 5.3%, $P = 0.001$). Lobes directly adjacent to the primary hemorrhagic contusion had a mean of 7.83 ± 7.51% atrophy, whereas the most remote lobes had a mean of 3.53 ± 3.26% atrophy ($P = 0.006$). Those patients with greater initial total hemorrhagic contusion volume experienced the greatest degree of chronic brain atrophy ($r = 0.62$, $P = 0.001$).

Univariate analysis for risk factors for regional or global brain atrophy showed that neither age, gender, initial GCS, percentage time $SJVO_2 < 50\%$, mean $SJVO_2$, nor CPP contributed significantly ($P > 0.15$ in all comparisons). Global atrophy was associated with elevated ICP, both for the cumulative duration of elevated ICP ($r = 0.59$, $P = 0.005$) and mean ICP ($r = 0.46$, $P = 0.028$) (Table 4). Those patients who required craniotomy to remove mass lesions ($n = 11$) had more severe global atrophy than did those who did not ($n = 21$) (10.4 ± 5.0% versus 6.3 ± 3.8%, $P = 0.033$). Figure 4 illustrates a case example of brain atrophy after TBI.

Acute TBI volumes were slightly but nonsignificantly larger than normal controls ($P = 0.272$). Chronic TBI brain volumes were significantly smaller than both controls ($P = 0.032$) and acute TBI volumes ($P = 0.013$); gray matter volumes were smaller than controls ($P = 0.022$). Cerebrospinal fluid volumes increased in chronic scans compared with acute scans ($P = 0.001$). There was no statistical difference between acute and chronic white matter volumes (Table 5). The extent of atrophy correlated poorly with the timing of MRI after TBI ($r = 0.04$, $P = 0.828$).

Table 4 Correlations between ICP and brain lobe atrophy

	Mean ICP		*Percentage time ICP > 20 mm Hg*	
	r	P-*value*	r	P-*value*
Temporal lobe	0.08	0.607	0.14	0.374
Frontal lobe	0.36	0.025	0.41	0.010
Parietal lobe	0.33	0.04	0.32	0.049
Occipital lobe	0.48	0.001	0.61	0.000
Global atrophy	0.46	0.034	0.59	0.005

ICP, intracranial pressure.
Correlations between and percentage atrophy by region.

Regional Metabolic Parameters Compared with Brain Atrophy

Regional measures of metabolism (CBF, OEF, $CMRO_2$, and CMRglc) were compared with regional atrophy using coregistered image analysis (Table 6**)**. Regional brain atrophy was correlated with $CMRO_2$ in the frontal ($P = 0.031$), temporal ($P = 0.001$), and parietal ($P = 0.006$) lobes. Regional atrophy was also corre-

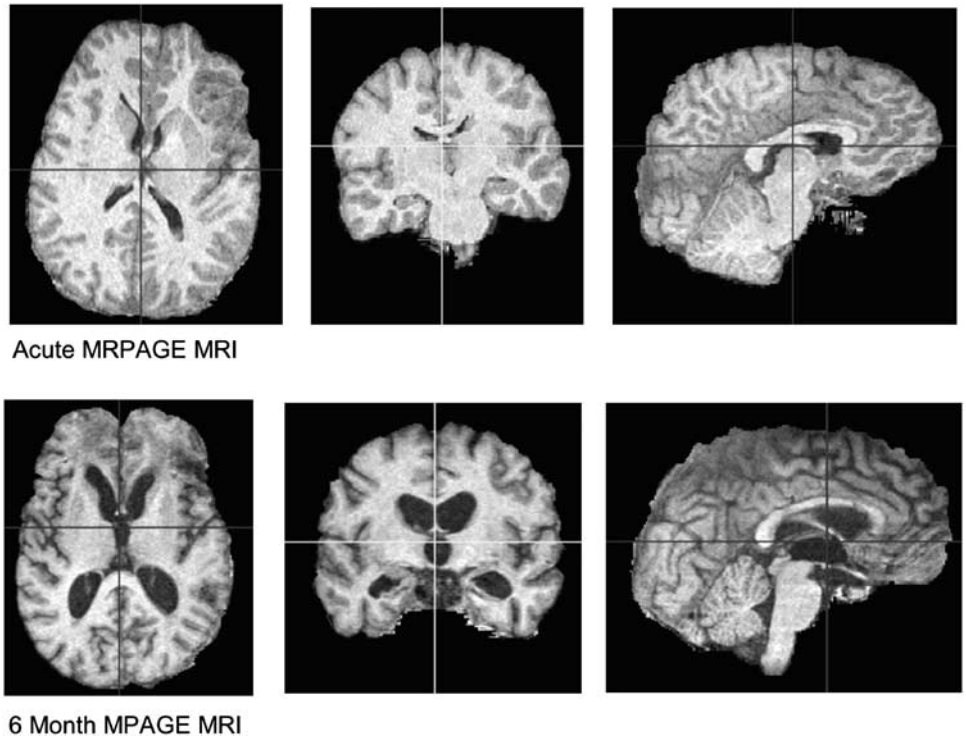

Figure 4 Example of chronic brain atrophy: Three-dimensional rendering of skull-stripped SPGR MRI T1 image in an example patient. The top row shows the acute MRI and the bottom row shows the chronic MRI at 6 months after trauma. The widespread atrophy, sulcal enlargement, and ventricular enlargement must be noted.

Table 5 Whole brain volume comparisons

	Whole brain volume	*Gray matter*	*White matter*	*CSF*
Normal control	1,274,834 (68,840)	663,305 (53,430)	611,529 (53,577)	192,253 (33,165)
TBI acute	1,327,595 (146,433)	688,142 (140,570)	673,800 (142,547)	202,205 (45,819)
TBI chronic	1,191,338 (102,441)†	582,457 (121,718)†	600,306 (129,354)	329,005 (78,139)‡

CSF, cerebrospinal fluid; TBI, traumatic brain injury.
The comparison of whole brain volumes of normal controls, acute TBI and chronic TBI samples (mean ± s.d.) is shown. Acute TBI brain volumes were similar ($P < 0.272$) to normal controls. Chronic TBI brain volumes were smaller than controls ($P < 0.013$)† and smaller than acute TBI volumes ($P < 0.022$)†, and gray matter volumes were smaller than controls ($P < 0.02$)†. CSF volumes increased in chronic scans as compared with acute TBI scans ($P < 0.001$)‡.

lated with CBF in the frontal ($P<0.001$), temporal ($P=0.001$), and parietal ($P=0.033$) lobes (Figures 5D–5F). Regional atrophy was correlated with CMRglc only in the frontal lobe ($P=0.004$). The OEF was not correlated to atrophy in any brain lobe. Atrophy in the occipital lobe did not correlate with any metabolic parameter.

Atrophy Compared with Neurologic Outcome

Regional lobar atrophy correlated poorly with GOS-e at 6 months. The specific correlations between atrophy and GOS-e were: temporal lobe ($r=-0.27$, $P=0.135$), frontal lobe ($r=-0.18$, $P=0.324$), parietal lobe ($r=-0.17$, $P=0.352$), and occipital ($r=0.09$, $P=0.624$) and global atrophy ($r=-0.27$, $P=0.135$).

Discussion

The principal findings of this study are as follows: (1) chronic brain atrophy occurred in all brain regions with the greatest atrophy in the temporal and frontal lobes and less atrophy in the occipital lobes; (2) the extent of brain atrophy was associated with the initial total volume of brain hemorrhage (either isolated contusions or combined diffuse axonal hemorrhagic injury); (3) widespread reduction in glucose and oxidative metabolism as measured by PET was seen, involving normal-appearing regions of the brain; (4) the extent of chronic brain atrophy correlated with nonischemic metabolic parameters regionally; and (5) regional irreversible brain ischemia was infrequently found on both PET OEF and MRI DWI-ADC imaging. These findings are novel and extend the body of

Table 6 Correlations between metabolism and brain lobe atrophy

Brain lobe	$CMRO_2$		CBF		CMRglc		OEF	
	r	P-*value*	r	P-*value*	r	P-*value*	r	P-*value*
Temporal lobe	−0.40	0.001*	−0.42	0.001*	−0.08	0.541	-0.03	0.805
Frontal lobe	−0.29	0.031*	−0.50	0.000*	−0.39	0.004*	0.13	0.335
Parietal lobe	−0.35	0.006*	−0.27	0.033*	−0.16	0.252	−0.18	0.165
Occipital lobe	−0.03	0.839	−0.04	0.775	−0.07	0.635	0.01	0.933

CBF, cerebral blood flow; CMRglc, cerebral metabolic rate of glucose; $CMRO_2$, cerebral metabolic rate of oxygen; OEF, oxygen extraction fraction.
Correlations between regional brain metabolism and percentage atrophy.
*$P < 0.05$.

knowledge regarding brain atrophy after TBI, highlighting the fact that atrophy is related to early brain metabolism, especially in normal-appearing brain tissue that was not primarily injured.

Brain Atrophy after Traumatic Brain Injury

Several longitudinal MRI studies have quantitatively examined progressive atrophy after TBI. The extent of atrophy varies among different studies according to the delay time from injury to imaging, the severity case mix, and the specific morphometry methods. MacKenzie *et al* (2002) reported a longitudinal change in the brain parenchymal volume of −4.16% on average compared with −1.49% in healthy controls. In that small study, the time from injury to the first scan varied between 7 and 430 days, thus conflating early and late atrophy. Trivedi *et al* (2007)published a study applying structural image evaluation, using normalization of atrophy (SIENA) (Smith *et al*, 2002) to evaluate global brain volume change between ~79 and 409 days after TBI in 37 patients with mild-to-severe TBI. The authors found a reduction in brain volume of 1.43% relative to healthy controls. In a recent longitudinal study, using a similar acute versus chronic within-subject design, Sidaros *et al* (2009) compared brain volumes at ~8 weeks and ~12 months after injury. The brain volume was already reduced by 8.4% on average in patients compared with controls, whereas a mean of 4.0% (median 2.9%) volume loss occurred in patients during the scan interval. This indicates that a decrease in brain volume occurs in the subacute period. In this study, acute and chronic MRI scans were performed 8 and 195 days, respectively, after trauma on average, and we found global brain atrophy with a mean of $7.8 \pm 7.2\%$. This result is similar to that of our previous study, also on voxel-based morphometry, which showed a mean tissue loss of $8.5 \pm 4.5\%$ in the whole brain (Marcoux *et al*, 2008). As the first MRI was performed in the acute period, it is possible that the clearing of brain edema over time might be responsible for some brain tissue volume loss. We attempted to control for this by comparing results with normal controls. Future studies should be conducted with multiple scan time points to better characterize the time course of progressive atrophy after TBI.

Our findings suggest spatial specificity of brain lobe atrophy after TBI. The temporal and frontal lobes showed greater atrophy than did occipital lobes. These findings are similar to the previous pediatric traumatic brain study (Wilde *et al*, 2005). The frontal and temporal lobes are among the areas most vulnerable to injury in TBI. Even after excluding contusion volumes from the calculation, the most frequently injured lobes displayed the greatest atrophy. The association between regional contusion size and regional atrophy in those areas containing contusions early on, and the correlation between total contusion volume and global brain atrophy suggest that atrophy is related to the immediate and/or prolonged effects of these contusions. Others have reported a dose-response effect of contusions on regional atrophy (Levine *et al*, 2008). As metabolic distress is the most severe in regions surrounding contusions (Vespa *et al*, 2007), atrophy may be due to regional metabolic distress. One speculation is that the cumulative local toxic effects of iron deposition may lead to oxidative stress and metabolic dysfunction, resulting in greater regional long-term global atrophy. A relationship between iron deposition and atrophy has been seen in primary intracerebral hemorrhage (Okauchi *et al*, 2009).

Metabolic Crisis After Traumatic Brain Injury is Correlated with Atrophy

The assumption that reduction in brain metabolism is well tolerated and benign is not supported by our data. The reduction in brain metabolism instead suggests that the tissue is in a metabolic crisis, despite the absence of markers of ischemia. Indeed, in a preliminary study, we used a combination of early PET imaging and longitudinal cerebral microdialysis monitoring to study metabolic disturbance in the acute period after trauma. In that study, we reported that the burden of microdialysis lactate–pyruvate ratio correlated negatively with $CMRO_2$ (Vespa *et al*, 2005). Factors responsible for global or regional brain atrophy have not been explored

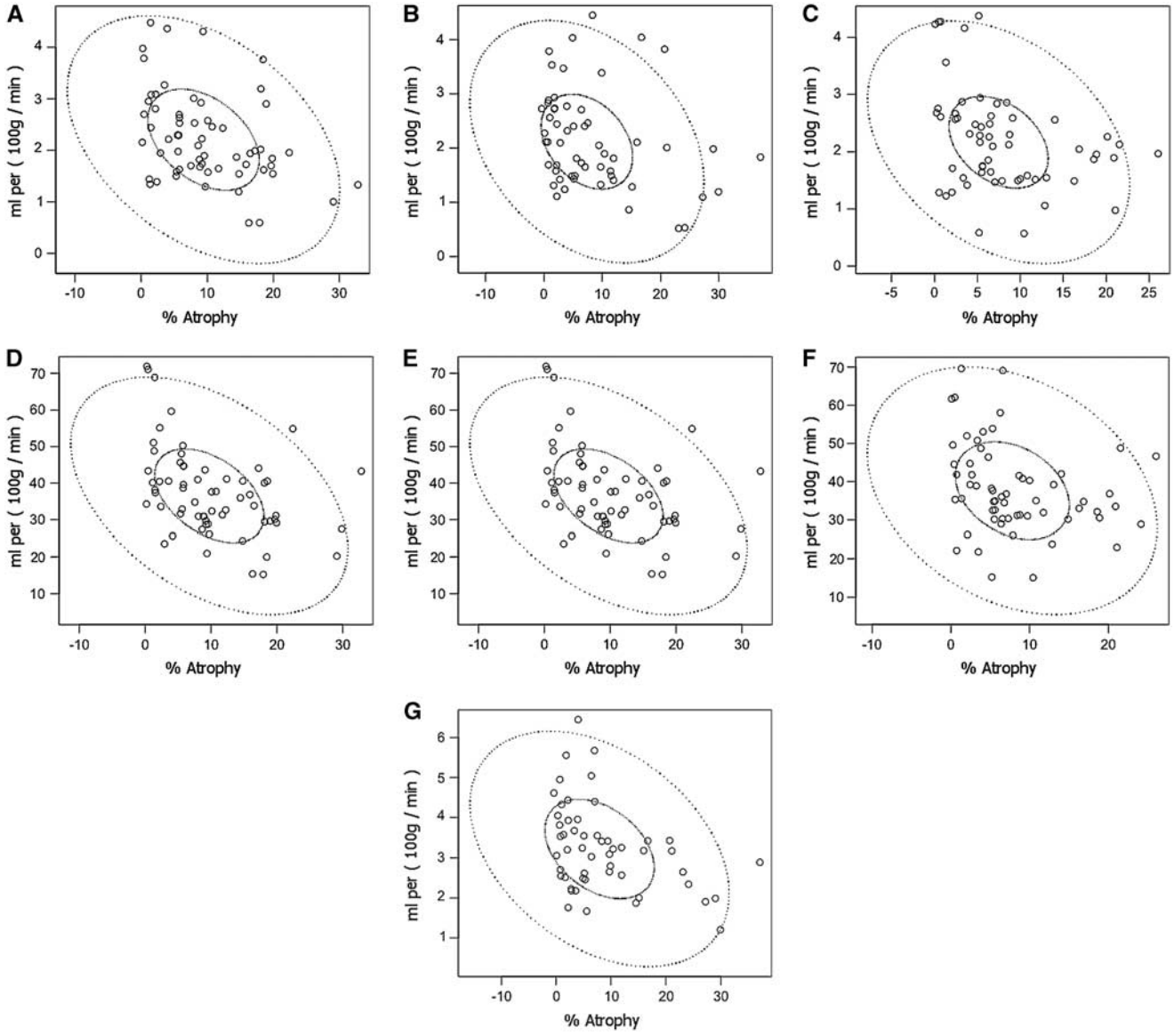

Figure 5 Correlations between $CMRO_2$ and atrophy in the temporal (**A**), frontal (**B**), and parietal lobes (**C**); between CBF and atrophy in the temporal (**D**), frontal (**E**), and parietal lobes (**F**); and between CMRglc and atrophy in the frontal lobe (**G**). The solid elliptical circles indicate the 50% confidence interval, and the dashed elliptical circle indicates the 99% confidence interval of the correlation coefficient.

in depth. On the basis of our previous finding that in the frontal lobe, persistent metabolic crisis as measured by elevated lactate–pyruvate ratio monitored by microdialysis is associated with tissue loss, we hypothesized that metabolic crises in other eloquent regions also correlate with tissue loss. Hence, areas of reduced $CMRO_2$ seen in this study may represent areas of the brain in metabolic crisis. The association of brain atrophy with reduced $CMRO_2$ offers further support to this hypothesis. The correlation between atrophy and elevated ICP lends indirect credence that the patients' brains were in distress. It is noteworthy that despite ICP elevation and the absence of irreversible ischemia on PET and MRI, long-term atrophy occurred in our study patients. Amplifying our previous microdialysis study by showing that the duration of regional metabolic crisis correlates with the extent of regional atrophy, this study provides information regarding the relationship between regional metabolism and regional atrophy in areas not monitored by microdialysis.

Our PET metabolic data are in agreement with our previous work (Wu *et al*, 2004). In this study, $CMRO_2$, CBF, and CMRglc were decreased in the acute period after trauma compared with normal healthy volunteers, but the OEF was similar to normals (Wu *et al*, 2004). In our current data, the OEF was similar in the nonischemic range. The pericontusional tissue does not display ischemia as

determined by the OEF in either our current data or in that of Wu *et al* (2004). Hence, our data do not support perilesional ischemia.

Most PET studies performed in TBI patients in the acute period after the injury have failed to show widespread brain ischemia. Coles *et al* (2004) reported finding ischemia in ~6% of whole brain volume overall, but a few patients had large volumes of ischemia associated with acute subdural hemorrhage. Our PET imaging was delayed in relation to imaging by Coles *et al*, and hence we may have missed early periods of ischemia. In our previous study combining PET and microdialysis in TBI patients, we found a lower mean ischemic brain volume, 1.5 cm^3, which translates into 1.5% of total brain volume; we also documented persistent and long-lasting evidence of metabolic crisis lasting several days despite the absence of brain ischemia. (Vespa *et al*, 2005). Positron emission tomography imaging conducted both at early time points and repeatedly over several days would be required to determine the presence of regional ischemia. As we were unable to do this, we instead used MRI DWI-ADC to complement our search for brain ischemia and found only a single patient with evidence of ischemia. Imaging performed by DWI-ADC provides a very sensitive and long-lasting marker for ischemia at any time after ischemic stroke. Presumably, even early ischemia occurring on postinjury day 1 would leave a lasting ischemic biomarker on DWI-ADC. Hence, MRI DWI-ADC may be more sensitive than PET in detecting ischemic damage. Our center has substantial experience using DWI-ADC to detect ischemic stroke. We see only limited DWI-ADC evidence of irreversible ischemia in this study. Our results are similar to other reports of TBI in which DWI-ADC lesions occur in conjunction with or independent of traumatic hemorrhage (Schaefer *et al*, 2004). By comparison, DWI-ADC lesions in this current cohort seem to be colocalized with brain hemorrhage and nearly all of DWI-ADC lesions detected were confined to areas of hemorrhage. Consequently, it seems that the primary lesion leading to metabolic dysfunction is a hemorrhagic lesion rather than an ischemic arterial occlusion lesion. Soustiel and Sviri (2007) have recently reported nonischemic metabolic dysfunction after TBI . In the most recent study by Coles *et al* (2009), using chronic MRI to characterize eventual tissue outcome, oxidative metabolism was reduced in both normal-appearing brain tissue, and contusions in the absence of ischemia. Therefore, the preponderance of available data suggests that reductions in brain metabolism are associated with nonischemic metabolic dysfunction rather than ischemia.

Limitations of the Study

Limitations of the study include its small sample size and cross-sectional design. This limitation, combined with a gross measure of chronic neurologic outcome, may have affected our ability to correlate atrophy with neurologic function. More specific cognitive testing that measures function of the frontal and temporal lobes might have provided a stronger correlation between atrophy and outcome. The brain tissue is often swollen during the initial week after TBI. However, we are reassured that brain volume calculations of acute MRI volumes were similar to age-matched controls. In addition, the percentage atrophy reported herein is similar to that in other studies of severe TBI. Hence, we do not believe that the observed atrophy is an artifact of acute brain edema. Conversely, the timing of chronic MRI in this study may have been too early to detect final changes, as atrophy appears to reach a maximum after 8 to 12 months and perhaps longer (Ng *et al*, 2008). The nature of traumatic lesions in patients may cause bias in the characteristics of lobe atrophy. Positron emission tomography is a snapshot examination and does not reveal long-term metabolic disturbance. Our PET imaging could have missed early ischemia. Ischemic changes may occur before or after PET. However, we coupled MRI ADC measures (to detect ultra-early ischemia that would show up as a stroke for many days) with continuous monitoring of brain oxygen (for detection of ischemia during the intensive-care period), to determine any possible occurrence of ischemia. We failed to detect ischemia as the major pathologic entity underlying the metabolic dysfunction using our current approach. It is noteworthy that normalization of ADC reduction occurs in large artery strokes treated with recanalization (Kidwell *et al*, 2000; Kidwell *et al*, 2002; Fiehler *et al*, 2002). The extent of the correction seems to be dependent on recanalization. Hence, this study may have missed early ADC reduction and thus early brain ischemia. However, this is a difficult issue as normalization of ADC after recanalization for ischemic stroke results in long-term tissue survival and not focal atrophy. Hence, a transient early ischemic event missed by our MRI imaging protocol would likely not contribute to the long-term atrophy that we report in this study. In some cases of ischemic stroke, the normalized ADC again becomes abnormal on MRI at day 7 after stroke despite early ADC normalization (Kidwell *et al*, 2000). Given that we imaged patients in a delayed manner in the acute setting (mean of 8 days), we theoretically would see late ADC signs of ischemia even if reperfusion had occurred after an early ischemic event. In contrast to our study, Menon and colleagues (Cunningham *et al*, 2005) have presented data indicating the importance of cellular edema, vascular compression, and microvascular ischemia leading to cellular injury; hence, our results are controversial. Overall, we acknowledge the potential of early ischemia after TBI, but to the best of our abilities, keeping the above experience in stroke ADC imaging in mind, we were not able to find substantive evidence of ischemia after TBI.

Conclusions

Chronic brain atrophy is regionally specific and is regionally associated with reductions in oxidative brain metabolism. The atrophy does not seem to be based on the occurrence of irreversible brain ischemia, as measured by PET and MRI DWI-ADC. Although the mechanisms leading to brain atrophy are as yet undetermined, the above- data suggest that impaired oxidative metabolism has a central role.

Disclosure/conflict of interest

The authors declare no conflict of interest.

References

Bergsneider M, Hovda DA, McArthur DL, Etchepare M, Huang SC, Sehati N, Satz P, Phelps ME, Becker DP (2001) Metabolic recovery following human traumatic brain injury based on FDG-PET: time course and relationship to neurological disability. *J Head Trauma Rehabil* 16:135–48

Coles JP, Cunningham AS, Salvador R, Chatfield DA, Carpenter A, Pickard JD, Menon DK (2009) Early metabolic characteristics of lesion and nonlesion tissue after head injury. *J Cereb Blood Flow Metab* 29:965–75

Coles JP, Fryer TD, Smielewski P, Rice K, Clark JC, Pickard JD, Menon DK (2004) Defining ischemic burden after traumatic brain injury using ^{15}O PET imaging of cerebral physiology. *J Cereb Blood Flow Metab* 24:191–201

Cunningham AS, Salvador R, Coles JP, Chatfield DA, Bradley PG, Johnston AJ, Steiner LA, Fryer TD, Aigbirhio FI, Smielewski P, Williams GB, Carpenter TA, Gillard JH, Pickard JD, Menon AK (2005) Physiological thresholds for irreversible tissue damage in contusional regions following traumatic brain injury. *Brain* 128:1931–42

Dinov ID, Van Horn JD, Lozev KM, Magsipoc R, Petrosyan P, Liu Z, MacKenzie-Graham A, Eggert P, Parker DS, Toga AW (2009) Efficient, distributed and interactive neuroimaging data analysis using the LONI pipeline. Front. *Neuroinform.* 3:22. doi:10.3389/neuro.11.022.2009, published online: 20 July 2009

Feeney DM, Baron JC (1986) Diaschisis. *Stroke* 17:817–30

Fiehler J, Foth M, Kucinski T, Knab R, von Bezold M, Weiller C, Zeumer H, Röther J (2002) Severe ADC decreases do not predict irreversible tissue damage in humans. *Stroke* 33:79–86

Goldberg KM, Iglewicz B (1992) Bivariate extensions of the boxplot. *Technometrics* 334:307–20

Hayman LA (1992) Adult cerebrum. In: *Clinical Brain Imaging: Normal Structure and Functional Anatomy* (Hayman LA and Hinck VC, eds), St Louis: Mosby Yearbook, 130–7

Kidwell CS, Saver JL, Mattiello J, Starkman S, Vinuela F, Duckwiler G, Gobin YP, Jahan R, Vespa P, Kalafut M, Alger JR (2000) Thrombolytic reversal of acute human cerebral ischemic injury shown by diffusion/perfusion magnetic resonance imaging. *Ann Neurol* 47:462–9

Kidwell CS, Saver JL, Starkman S, Duckwiler G, Jahan R, Vespa P, Villablanca JP, Liebeskind DS, Gobin YP, Vinuela F, Alger JR (2002) Late secondary ischemic injury in patients receiving intraarterial thrombolysis. *Ann Neurol* 52:698–703

Langlois JA, Kegler SR, Butler JA, Gotsch KE, Johnson RL, Reichard AA, Webb KW, Coronado VG, Selassie AW, Thurman DJ (2003) Traumatic brain injury-related hospital discharges. *MMWR Surveill Summ* 52:1–20

Levin HS, Benavidez DA, Verger-Maestre K, Perachio N, Song J, Mendelsohn DB, Fletcher JM (2000) Reduction of corpus callosum growth after severe traumatic brain injury in children. *Neurology* 54:647–53

Levine B, Kovacevic N, Nica EI, Cheung G, Gao F, Schwartz ML, Black SE (2008) The Toronto traumatic brain injury study: injury severity and quantified MRI. *Neurology* 70:771–8

Lin K, Huang S, Baxter L, Phelps M (1994) A general technique for inter-study registration of multi-function and multimodality images. *IEEE Trans Nucl Sci* 41: 2850–5

Marcoux J, McArthur DA, Miller C, Glenn TC, Villablanca P, Martin NA, Hovda DA, Alger JR, Vespa PM (2008) Persistent metabolic crisis as measured by elevated cerebral microdialysis lactate-pyruvate ratio predicts chronic frontal lobe brain atrophy after traumatic brain injury. *Crit Care Med* 36:2871–7

MacKenzie JD, Siddiqi F, Babb JS, Bagley LJ, Mannon LJ, Sinson GP, Grossman RI (2002) Brain atrophy in mild or moderate traumatic brain injury: a longitudinal quantitative analysis. *AJNR Am J Neuroradiol* 23: 1509–1515

Ng K, Mikulis DJ, Glazer J, Kabani N, Till C, Greenberg G, Thompson A, Lazinski D, Agid R, Colella B, Green D (2008) Magnetic resonance imaging evidence of progression of subacute brain atrophy in moderate to severe traumatic brain injury. *Arch Phys Med Rehabil* 89: S35–44

Ohta S, Meyer E, Thompson CJ, Gjedde A (1992) Oxygen consumption of the living human brain measured after a single inhalation of positron emitting oxygen. *J Cereb Blood Flow Metab* 12:179–92

Okauchi M, Hua Y, Keep RF, Morgenstern LB, Xi G (2009) Effects of deferoxamine on intracerebral hemorrhage-induced brain injury in aged rats. *Stroke* 40:1858–63

Press WH, Flannery BP, Teukolsky SA, Vettering WT. Numerical recipes. *The Art of Scientific Computing*. Cambridge, MA: Cambridge University Press, 1986

Schaefer PW, Huisman TA, Sorensen AG, Gonzalez RG, Schwamm LH (2004) Diffusion-weighted MR imaging in closed head injury: high correlation with initial Glasgow Coma Scale score and score on modified Rankin scale at discharge. *Radiology* 233:58–66

Shattuck DW, Leahy RM (2002) BrainSuite: an automated cortical surface identification tool. *Med Image Anals* 8:129–42

Sidaros A, Skimminge A, Liptrot MG, Sidaros K, Engberg AW, Herning M, Paulson OB, Jernigan TL, Rostrup E (2009) Long-term global and regional brain volume changes following severe traumatic brain injury: a longitudinal study with clinical correlates. *Neuroimage* 44:1–8

Smith SM, Zhang Y, Jenkinson M, Chen J, Matthews PM, Federico A, De Stefano N (2002) Accurate, robust, and automated longitudinal and cross-sectional brain change analysis. *Neuroimage* 17:479–89

Soustiel JF, Sviri GE (2007) Monitoring of cerebral metabolism: non-ishchemic impairment of oxidative metabolism following severe traumatic brain injury. *Neurol Res* 29:654–60

Tate DF, Bigler ED (2000) Fornix and hippocampal atrophy in traumatic brain injury. *Learn Mem* 7:442–6

Trivedi MA, Ward MA, Hess TM, Gale SD, Dempsey RJ, Rowley HA, Johnson SC (2007) Longitudinal changes in global brain volume between 79 and 409 days after traumatic brain injury: relationship with duration of coma. *J Neurotrauma* 24:766–71

Verger K, Junqué C, Levin HS, Jurado MA, Pérez-Gómez M, Bartrés-Faz D, Barrios M, Alvarez A, Bartumeus F, Mercader JM (2001) Correlation of atrophy measures on MRI with neuropsychological sequelae in children and adolescents with traumatic brain injury. *Brain Inj* 15:211–21

Vespa P, Bergsneider M, Hattori N, Wu HM, Huang SC, Martin NA, Glenn TC, McArthur DL, Hovda DA (2005) Metabolic crisis without brain ischemia is common after traumatic brain injury: a combined microdialysis and positron emission tomography study. *J Cereb Blood Flow Metab* 25:763–74

Vespa PM, Miller C, McArthur D, Eliseo M, Etchepare M, Hirt D, Glenn TC, Martin N, Hovda D (2007) Non-convulsive electrographic seizures after traumatic brain injury result in a delayed, prolonged increase in intracranial pressure and metabolic crisis. *Crit Care Med* 35:2830–6

Wilcox RR (2005) *Introduction to Robust Estimation and Hypothesis Testing*. New York, NY: Elsevier

Wilde EA, Hunter JV, Newsome MR, Scheibel RS, Bigler ED, Johnson JL, Fearing MA, Cleavinger HB, Li X, Swank PR, Pedroza C, Roberson GS, Bachevalier J, Levin HS (2005) Frontal and temporal morphometric findings on MRI in children after moderate to severe traumatic brain injury. *J Neurotrauma* 22:333–44

Wilson JT, Pettigrew LE, Teasdale GM (1998) Structured interviews for the Glasgow Outcome Scale and the extended Glasgow Outcome Scale: guidelines for their use. *J Neurotrauma* 15:573–85

Wu HM, Huang SC, Hattori N, Glenn TC, Vespa PM, Hovda DA, Bergsneider M (2004) Subcortical white matter metabolic changes remote from focal hemorrhagic lesions suggest diffuse injury after human traumatic brain injury. *Neurosurgery* 55:1306–15; discussion 1316–1317

Yount R, Raschke KA, Biru M, Tate DF, Miller MJ, Abildskov T, Gandhi P, Ryser D, Hopkins RO, Bigler ED (2002) Traumatic brain injury and atrophy of the cingulated gyrus. *J Neuropsychiatry Clin Neurosci* 14:416–23